Journal of the Taiwan Institute of Chemical Engineers 74 (2017) 225–232

Contents lists available at ScienceDirect

Journal of the Taiwan Institute of Chemical Engineers

journal homepage: www.elsevier.com/locate/jtice

Ozonation enhancement by Fe–Cu biometallic particles

Teresa Torres-Blancas[c], Gabriela Roa-Morales[a,*], Fernando Ureña-Núñez[b], Carlos Barrera-Díaz[a], Alejandro Dorazco-González[c], Reyna Natividad[a,*]

[a] Centro Conjunto de Investigación en Química Sustentable CCIQS UAEM-UNAM, Facultad de Química, Universidad Autónoma del Estado de México (UAEMex), Carretera Toluca-Atlacomulco, km 14.5, C.P. 50200 Toluca, México

[b] Instituto Nacional de Investigaciones Nucleares, km 36.5, Carretera México-Toluca, Ocoyoacac, Estado de México C.P.52750, México

[c] Centro Conjunto de Investigación en Química Sustentable, UAEM-UNAM, C. P. 50200, Toluca, Estado de México, México. Instituto de Química, Universidad Nacional Autónoma de México

ARTICLE INFO

Article history:
Received 4 October 2016
Revised 19 January 2017
Accepted 24 February 2017
Available online 23 March 2017

Keywords:
AOPs
Bimetallic particles
Dye, indigo carmine
Fenton
Fenton-like

ABSTRACT

The aim of this work was to assess the effect of the bimetallic system Fe–Cu on the ozonation efficiency of indigo carmine and its main degradation product, isatin-5-sulfonic acid. As reference, experiments with single metal particles were also conducted. The metallic systems were synthesized by a chemical reduction method and characterized by EPR and HR-SEM/EDS. Cu and Fe oxidation states were found to be 2^+. The ozonation process was carried out in an up-flow bubble column. The organic compounds concentration was determined by UV–vis spectroscopy. The degree of oxidation and mineralization was determined by COD and TOC measurements, respectively. The effect of pH was also studied. It was found that the use of the bimetallic system not only considerably (by three times) improves the ozonation rate but also the mineralization degree of indigo carmine. The best results (97% indigo carmine removal and 92% of TOC removal) were obtained at pH 3 and with 1000 mg/l of Fe/Cu particles.

1. Introduction

A vast amount of water is employed by the textile industry. In the dyeing process, the produced wastewater contains strong color, which is reflected in a high chemical oxygen demand (COD). It has been estimated that 1–15% of the dye is lost during dyeing and finishing processes and it is released in the wastewater [1–3]. The discharge of effluents into the environment containing reactive dyes can interfere with sunlight transmission into flowing streams [4–7]. Available techniques for removing dyes have been studied as photodegradation [8], adsorption filtration [9], coagulation and biological treatments [10]. However, the stability of the organic molecules present in the dyes is high, and some of these methods are not completely effective. Therefore, recent progress on water treatment based on the chemical oxidation of organic compounds by advanced oxidation processes (AOPs) like ozonation have drawn attention [11]. Ozonation, which is effective, versatile, and environmentally sound, has been proved to be in recent years a good method for color removal. Ozone is a strong oxidant ($E^\circ = 2.07$ V) and reacts rapidly with most organic compounds degrading them [12,13]. In AOPs hydroxyl radicals ($^\bullet$OH) are used as oxidant, which is capable of oxidizing almost any organic substance. The fundamental feature of the radical is the existence of a single electron, instead of a free electron pair. This electron makes the $^\bullet$OH radical highly reactive. The oxidation of organic substances takes place in stages, with formation of intermediates, due to the high stability of organic molecules present in the dye-products. In the case of organics' complete oxidation, these are transformed into inorganic end products, water and carbon dioxide or mineralization of the molecule [14,15]. In spite of more efficient processes, the catalyzed ozonation has been successfully studied. In this sense, bimetallic systems have emerged as promising catalysts for environmental remediation. Their strong reducing ability can be used to remove numerous environmental pollutants (*e.g.*, heavy metals, halogenated organic compounds, nitro and azo compounds, and oxyanions) [16–19]. As a new class of materials comprising two different metals, bimetallic particles or metal oxides exhibit new functionalities because of synergy rather than merely additive effects of the metals [20–22]. In this work, the effect of adding metallic (Fe and Cu) and bimetallic particles (Fe–Cu) on the ozonation process efficiency is assessed. Indigo carmine and its main degradation product isatine-5-sulfonic acid [23–25], were elected as model molecules. The indigo carmine dye is widely and mainly used in the textile industry for denim dyeing.

* Corresponding authors.
E-mail addresses: therezabtt@gmail.com (T. Torres-Blancas), groam@uaemex.mx (G. Roa-Morales), reynanr@gmail.com (R. Natividad).

http://dx.doi.org/10.1016/j.jtice.2017.02.025
1876-1070/

2. Materials and methods

2.1. Reagents

Sulfuric acid, sodium hydroxide, iron sulfate (II), copper sulphate (II), indigo carmine dye (IC), isatin5-sulfonic acid (ISA) and sodium borohydride analytical grade were purchased from Sigma-Aldrich Chemicals. 0.1 M solutions of the acid and the base were used without further purification to adjust the solutions pH to 3, 5 and 7. Ozone was generated *in situ* from dry air by an ozone generator (Pacific Ozone Technology), with an average production of 0.005 g/l.

2.2. Synthesis of Fe, Cu and Fe/Cu particles

In order to synthesize the binary Fe/Cu system, 250 ml of 0.01 M iron sulfate (II) solution and 250 ml of 0.01 M copper sulfate were mixed in a beaker at 300 rpm using glass stirrers. The solution pH was adjusted by the dropwise addition of 0.5 M NaOH solution. The pH was monitored with a potentiometer (15 Conductronic Digital pH–mV–pH–Meter °C). Subsequently and in concordance with reaction 1 [26] the chemical reduction of the particles was conducted by adding an excess (1.1 M, 100 ml) of sodium borohydride solution under a nitrogen atmosphere. The black colored precipitate was further stirred 15 min and this was followed by vacuum filtration through a 0.2 mm cellulose acetate filter paper. The borohydride in excess was removed with ethanol and acetone. The Fe and Cu particles were synthesized in a similar manner albeit separately under similar conditions.

$$2Fe^{2+} + 2Cu^{2+} + 2H_2O + BH_4^- + 4e^- \rightarrow 2Fe(Cu)_{(s)} + BO_2^- + 4H^+ + 2H_{2(g)} \quad \text{(reaction 1)}$$

2.3. Ozonation experiments

The ozonation experiments were conducted in a 1 l up-flow glass bubble column reactor. Ozone was continuously produced by an ozone generator and was fed through a 2 µm pore size gas diffuser at the lower part of the reactor. The effect of three materials (Cu, Fe and Fe/Cu particles) on the ozonation process efficiency was assessed. The effect of pH was also studied in the range of 3–7. At all experiments the indigo carmine (IC) initial concentration was 500 mg/l. As control experiments, IC concentration profiles were established by adsorption and by ozonation alone. For the adsorption experiment, only particles without any ozone supply were employed in order to discard the removal of IC by physical means. To avoid discharging ozone to the atmosphere, the unreacted ozone was trapped and destroyed in a heated catalytic ozone destroyer (Pacific Technology d41202). Samples were taken at specific time intervals to be analyzed by different techniques (UV–vis spectrophotometry, TOC and COD). All experiments were carried out at 288 K.

2.4. Characterization of Fe, Cu and Fe/Cu particles

2.4.1. High resolution scanning electron microscopy (HR-SEM/EDS)

Micrographs were obtained in a JEOL JSM 6510LV instrument at 15 kV with 10 mm WD using both secondary and backscattered electron signals. The metallic particles samples were coated with a 20 nm gold thin film using a Denton Vacuum DESK IV sputtering equipment with a gold target.

2.4.2. Electron paramagnetic resonance (EPR)

EPR measurements were conducted in a quartz tube at 77 K with a JES-TE300 JEOL spectrometer operating at X- band fashions at 100 KHz modulation frequencies and a cylindrical cavity in the TE_{011} mode. The external calibration of the magnetic field was made with a precision gauss meter JEOL ES-FC5. Spectral acquisition and manipulations were performed using the program ES-IPRITS/TE. The EPR spectrum was recorded as a first derivation and the main parameter such as *g*-factor values were calculated according to Wertz [27].

2.5. Chemical analysis

The concentration of indigo carmine was determined by UV–vis spectrophotometry by using a Perkin Elmer Model Lambda 25 UV–vis spectrophotometer with a wavelength range of 190–1000 nm. The samples were scanned at a rate of 960 nm/s in a quartz cell with 1 cm optical path. The samples absorbance was scanned at wavelengths from 200 to 900 nm. A maximum absorbance of IC at 610 nm was observed and for isatin5-sulfonic acid a maximum absorbance at 303 nm was determined. This was corroborated with the corresponding standards. All experiments were carried out at room temperature (19 °C ± 2). In addition, to determine the degree of mineralization of indigo carmine, total organic carbon (TOC) analyses were performed in a Shimadzu analyzer TOC-LCPH/CPN and chemical oxygen demand (COD) of the samples was determined using the American Public Health Association (APHA) standard procedures [28].

3. Results and discussion

3.1. Characterization

3.1.1. HR-SEM/EDS of Fe, Cu and Fe/Cu particles

Fig. 1 presents a SEM/EDS image of prepared Fe, Cu and Fe/Cu particles, before reaction with IC. It can be observed that Fe and Cu particles are spherical in nature (size 50–90 × 10^{-3} µm) and connected together forming cumulus, as shown in Fig. 1a and b. The SEM/EDS image of Fe/Cu (Fig. 1c) shows particles also forming a chain most probably due to the magnetic interaction between particles [29], which causes the rapid reduction rate of metal ions, in all cases.

3.1.2. Electron paramagnetic resonance (EPR)

In order to determine the oxidation state of Cu and Fe in the synthesized materials before and after their use in the ozonation process, X-band EPR spectra of Cu, Fe and bimetallic Cu/Fe particles were recorded at 77 K (Fig. 2). The presence and oxidation state of Cu(II) atoms could be easily identified because only Cu(II) (electronic configuration $3d^9$, $S = 1/2$) is active at this spectroscopy. The EPR spectra of Cu particles before and after their use in the ozonation process are almost symmetrical singlets (Fig. 2a) with isotropic *g* values of 2.394025 and 2.39001, respectively, which are typical of Cu(II) [27,28]. The absence of the superfine lines and a broad shape signal is explained by the fast rotation of particles in water and interparticle interactions, which results in an isotropic g tensor [28]. On the other hand, samples containing fresh Fe particles (before being used in the ozonation process) are EPR silent indicating a oxidation state +2. Interestingly, after degradation, these samples show a typical broad signal of Fe(III) with isotropic $g = 3.11152$ (electronic configuration $3d^5$, $S = 3/2$) (Fig. 2b). Fig. 2c shows the EPR spectra of bimetallic Fe/Cu samples. The spectrum of these particles prior their use in the ozonation process shows a signal with axial symmetry with two *g* values, the first high intensity band around $g = 2.18023$ and a less intense one at $g = 2.2034$. There are not observed signals that correspond to Fe(III) atoms in this spectrum. The *g* values follow the order $g_\perp > g_\parallel > 2.1823$ [30]. These values are rather characteristic of Cu(II) ions forming CuO clusters located in octahedral sites [38]. In contrast, the EPR spectrum of the used Fe/Cu particles shows two broad overlapping

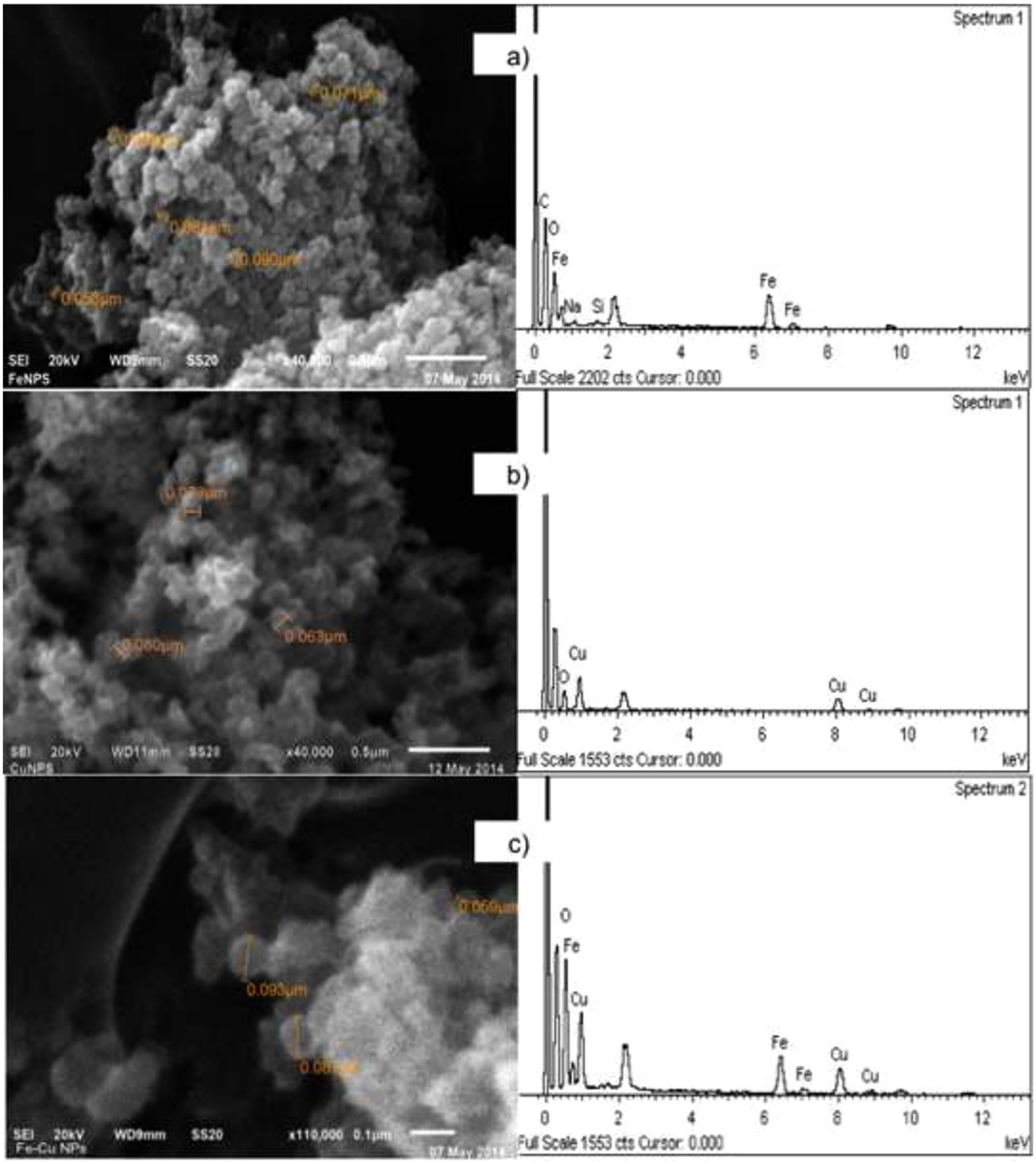

Fig. 1. SEMEDS images of (a) Fe, (b) Cu and (c) FeCu particles.

bands. The first signal with isotopic value of $g = 2.08196$ indicates the presence of Cu(II) atoms and the second less intense signal with $g = 3.3398$ can be attributed to Fe(III) ions with intermediate spin state $S = 3/2$. From this spectrum is difficult to determine whether there is an interaction Fe(III)/Cu(II), the only clear conclusion is the presence of Cu(II) and Fe(III) in the already used material [38]. It is also worth pointing out that by this technique the presence of Fe(II) is acknowledged prior use and cannot be disregarded in the spent material.

3.2. UV–vis spectra of IC and isatin 5-sulfonic acid

Fig. 3 shows the characteristic UV–vis spectra of ICand ISA standards at 10 mg/l. In this figure, the observed maximum absorption band at 610 nm is characteristic of IC and is ascribed to auxochromes (N, SO_3) together with the benzene ring [12]. It can also be observed that the characteristic ISA UV–vis spectrum exhibits a maximum of absorbance at 304 nm.

3.3. Ozonation

3.3.1. Effect of Fe, Cu or Fe/Cu addition

The effect of adding Fe, Cu or Fe/Cu particles on the removal of IC by ozonation was studied and followed by UV–vis spectrophotometry. For this purpose, two types of experiments were performed. One set of experiments was conducted only with the metallic system (without adding ozone) and another type of experiments was conducted with ozone plus metallic particles. The former was performed in order to verify the amount of IC removed by adsorption with each metallic system. It was found that the maximum removal of IC by adsorption was 5.2, 4.2 and less than 2.0% by the Fe/Cu, Fe and Cu particles, respectively, after 60 min. Therefore, it can be concluded that the effect of adding a

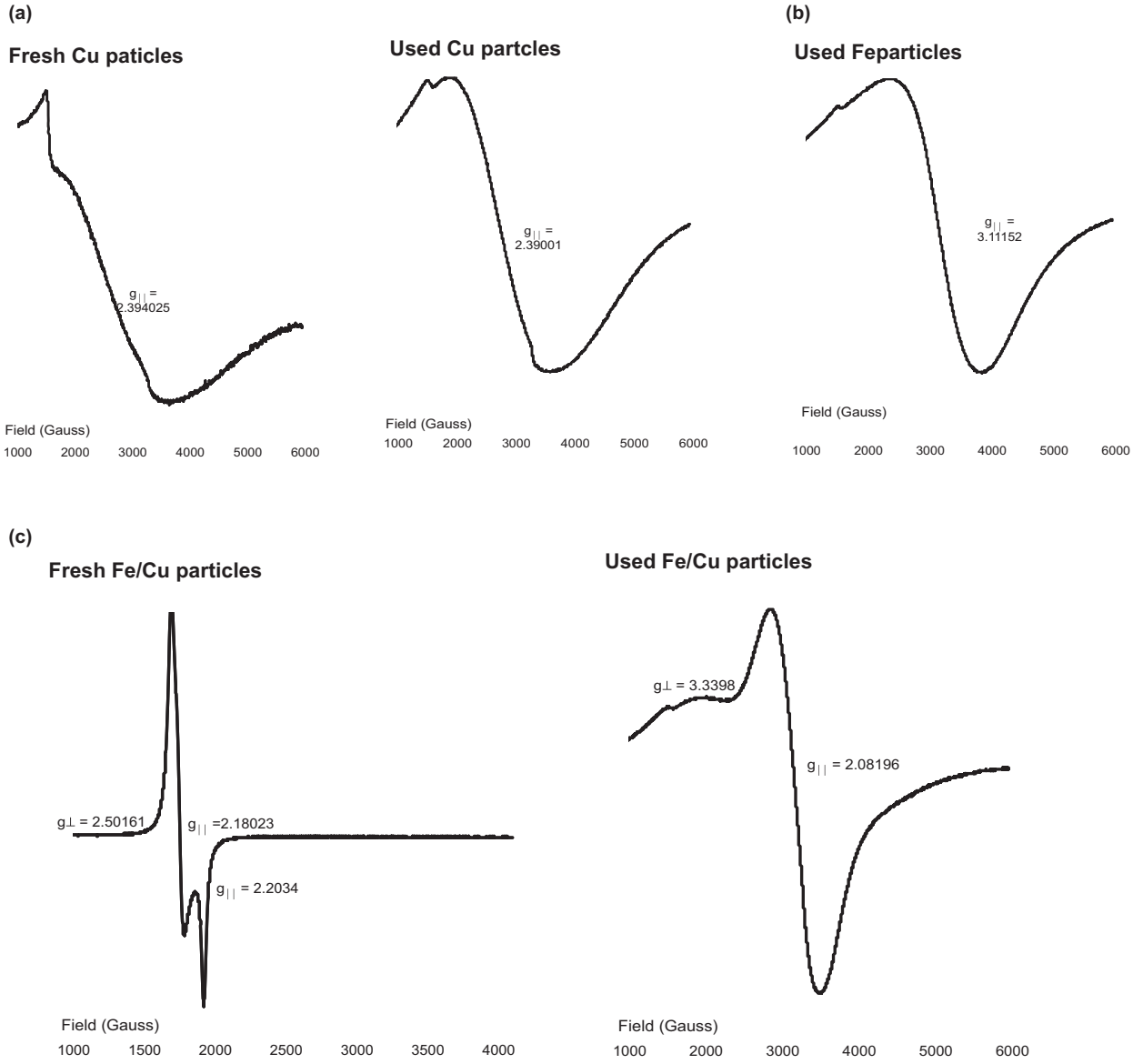

Fig. 2. EPR spectra of fresh and used.

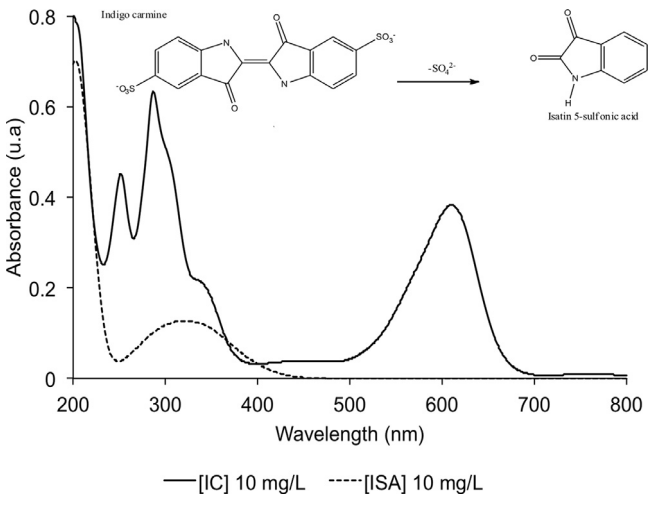

Fig. 3. UV–vis spectra of IC.

metallic system alone on the removal of IC is not significant .Regarding the ozonation process, Fig. 4 shows the samples UV–vis spectra after 60 min of ozonation under pH = 3 when Fe, Cu or Fe/Cu particles are added (1000 mg/l) to the process. By comparing the absorbance at 610 nm, it can be observed that within 60 min of reaction, ozonation alone does not fully remove the IC, since only 58% removal is achieved. However, when Fe, Cu or Fe/Cu particles are added to the reaction system, the absorbance at 610 nm is substantially diminished. Actually, according to the UV–vis spectra depicted in Fig. 4 when adding Fe or Cu particles, the IC removal efficiency was 60 and 70%, respectively. Also, it is worth noticing that the use of the bimetallic system implies a substantial enhancement of the IC removal (97%).The positive effect of the addition of metallic particles to the ozonation system can be ascribed to the improvement of the ozone decomposition. When the removal of IC is by ozonation only, the generation of free oxidant radicals and hydrogen peroxide is expected through reactions 2, 3 and 6 [31]. Therefore, the oxidation of the IC molecule is likely to occur via direct oxidation by the ozone molecule and by the free hydroxyl (•OH) and hydroperoxyl ($HO_2^{\bullet}$) radicals generated in

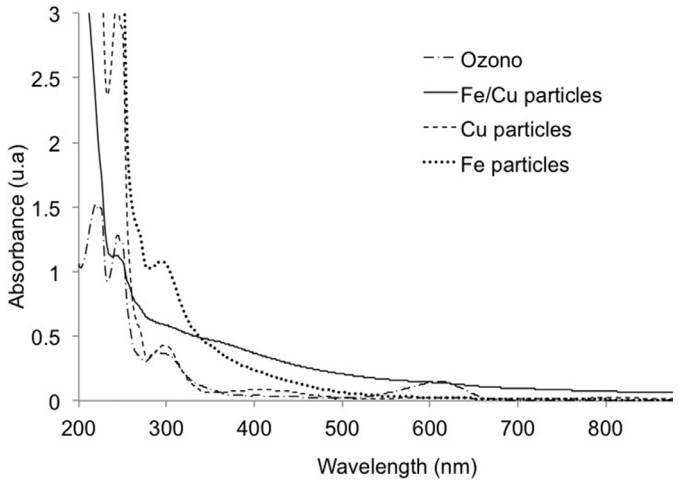

Fig. 4. Effect of catalyst on samples UV–vis spectra.

reactions 2 and 6 [32]. Concomitantly, these radicals are either consumed by the oxidation of IC or in the production of hydrogen peroxide and superoxide anion (reactions 4 and 5) [15,32]. This anion leads to the further production of both hydrogen peroxide and hydroxyl radicals (reactions 7 and 8).

$$2O_3 + H_2O \rightarrow HO^{\bullet} + 2O_2 + HO_2^{\bullet} \quad \text{(reaction 2)}$$

$$O_3 + 3H_2O \rightarrow 3H_2O_2 \quad \text{(reaction 3)}$$

$$\frac{1}{2}H_2O + HO^{\bullet} \rightarrow H_2O_2 \quad \text{(reaction 4)}$$

$$HO_2^{\bullet} \leftrightarrow O_2^{\bullet -} + H^+ \quad \text{(reaction 5)}$$

$$H_2O_2 \rightarrow HO_2^{\bullet} + H^+ \quad \text{(reaction 6)}$$

$$2O_2^{\bullet -} + 2H^+ \rightarrow H_2O_2 + O_2 \quad \text{(reaction 7)}$$

$$O_2^{\bullet -} + H_2O_2 \rightarrow HO^{\bullet} + HO^- + O_2 \quad \text{(reaction 8)}$$

Once the hydrogen peroxide is formed then the peroxonation process may be also occurring [31]. During this process the anion (HO_2^-) is formed in reaction 9 and reacts with ozone to either produce the hydroperoxyl radical (reaction 10) or an aduct (reaction 11) that has been reported [31] to be vital for the formation of the anion $O_3^{\bullet -}$ (reaction 12). The presence of this anion is important since further participates in the production of hydroxyl radicals via reaction 13.

$$H_2O_2 \leftrightarrow HO_2^- + H^+ \quad \text{(reaction 9)}$$

$$HO_2^- + O_3 \leftrightarrow HO_2^{\bullet} + O_3^{\bullet -} \quad \text{(reaction 10)}$$

$$HO_2^- + O_3 \leftrightarrow HO_5^- \quad \text{(reaction 11)}$$

$$HO_5^- \leftrightarrow HO_2^{\bullet} + O_3^{\bullet -} \quad \text{(reaction 12)}$$

$$O_3^{\bullet -} + H^+ \leftrightarrow HO_3 \rightarrow HO^{\bullet} + O_2 \quad \text{(reaction 13)}$$

When Fe^{2+} is introduced, it enhances ozone decomposition to produce additional •OH radicals either through the reaction with $O_3^{\bullet -}$ anion (reactions 13–15) or through the formation of $(FeO)^{2+}$ (reaction 15) [33]. Regarding Cu, there is an intermediate reaction to promote the generation of free radicals via reaction 17 [34]. It is worth pointing out that reaction 17 has been recently reported [34] and only theoretically demonstrated.

$$O_3 + Fe^{2+} \rightarrow O_3^{\bullet -} + Fe^{3+} \quad \text{(reaction 14)}$$

$$O_3 + Fe^{3+} \rightarrow FeO^{2+} + O_2 \quad \text{(reaction 15)}$$

$$O_3 + 3Cu^+ + 6H^+ \rightarrow 3H_2O + 3Cu^{2+} \quad \text{(reaction 16)}$$

$$[CuO]_n^+ + O_3 + H_2O \rightarrow 2HO^{\bullet} + O_2 + [CuO]_n \quad \text{(reaction 17)}$$

In addition to the aforementioned reactions, the production of oxidant radicals, •OH and or $HO_2^{\bullet}$ (reaction 24), via Fenton (18–21) and Fenton-like reactions (22–23) cannot be neglected since a substantial improvement of IC degradation is observed when metallic particles are added to the ozonation process [35]. Therefore, the catalytic effect of these materials should be acknowledged.

$$Fe^{2+} + H_2O_2 \rightarrow 2HO^{\bullet} + Fe^{3+} \quad \text{(reaction 18)}$$

$k_{19} = 70\ M^{-1}s^{-1}$ [36]

$$Fe^{3+} + H_2O_2 \rightarrow H^+ + HO_2^{\bullet} + Fe^{2+} \quad \text{(reaction 19)}$$

$k_{20} = 0.001 - 0.01\ M^{-1}s^{-1}$[36]

$$Fe^{2+} + HO^{\bullet} \rightarrow HO^- + Fe^{3+} \quad \text{(reaction 20)}$$

$k_{21} = 3.2 \times 10^8\ M^{-1}s^{-1}$[36]

$$Fe^{3+} + HO_2^{\bullet} \rightarrow Fe^{2+} + H^+ + O_2 \quad \text{(reaction 21)}$$

$k_{22} = 1.2 \times 10^6 M^{-1}s^{-1}$[35]

$$Cu^{2+} + H_2O_2 \rightarrow HO_2^{\bullet} + H^+ + Cu^+ \quad \text{(reaction 22)}$$

$k_{23} = 4.6 \times 10^2 M^{-1}s^{-1}$[37]

$$Cu^+ + H_2O_2 \rightarrow Cu^{2+} + HO^{\bullet} + HO^- \quad \text{(reaction 23)}$$

$k_{24} = 1 \times 10^4 M^{-1}s^{-1}$[34]

$$HO^{\bullet} + HO^{\bullet} \rightarrow H_2O_2 \quad \text{(reaction 24)}$$

$k_{25} = 4.2 \times 10^8 M^{-1}s^{-1}$[35]

$$Fe^{2+} + Cu^{2+} + 3H_2O_2 \rightarrow 3HO^{\bullet} + HO_2^{\bullet} + H_2O + Fe^{3+} + Cu^{2+} \quad \text{(reaction 25)}$$

$$C_{16}H_8N_2O_8S_2^{2-} + 28H_2O \rightarrow 16CO_2 + 2NH_4^+ + 2SO_2 + 56H^+ \quad \text{(reaction 26)}$$

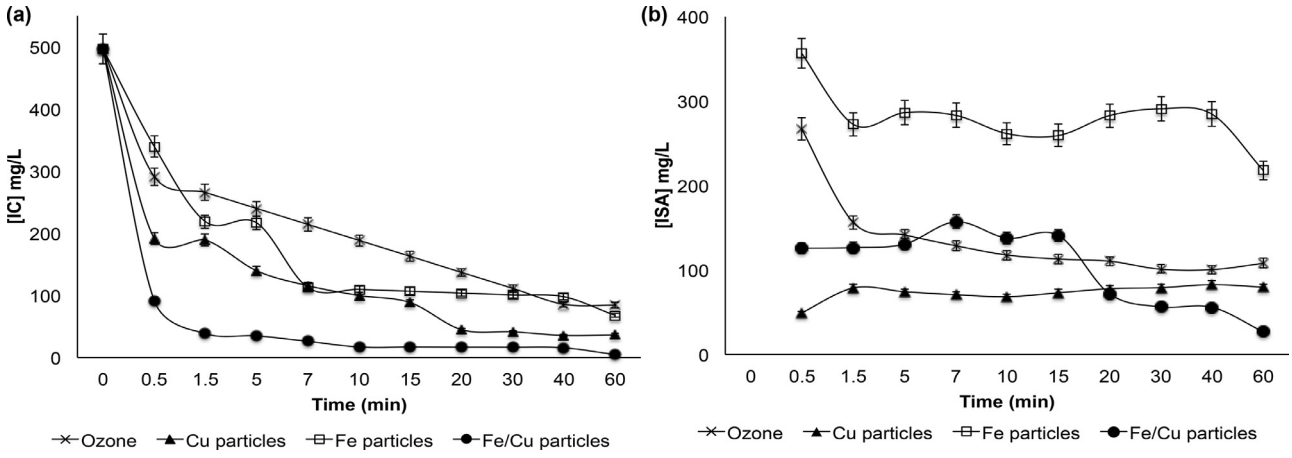

Fig. 5. Effect of catalyst (Fe, Cu and FeCu particles).

Table 1
Effect of the addition of metallic particles to the ozonation process on the IC initial oxidation rate.

Treatment	Only O_3	Cu	Fe	Fe/Cu
$-r_{IC0}$ **(mol/dm^{3}s)x10^6**	2.40	4.1	1.9	8.00

Table 2
Analysis of total organic carbon in the materials used as catalysts.

	Total carbon	Organic carbon mg/l	Inorganic carbon
[IC] = 500 mg/l	206 ± 5	202 ± 5	4 ± 5
Ozone (60 min)	58 ± 5	55 ± 5	3 ± 5
Fe (60 min)	82 ± 5	80 ± 5	3 ± 5
Cu (60 min)	40 ± 5	38 ± 5	3 ± 5
Fe/Cu (60 min)	16 ± 5	13 ± 5	2 ± 5

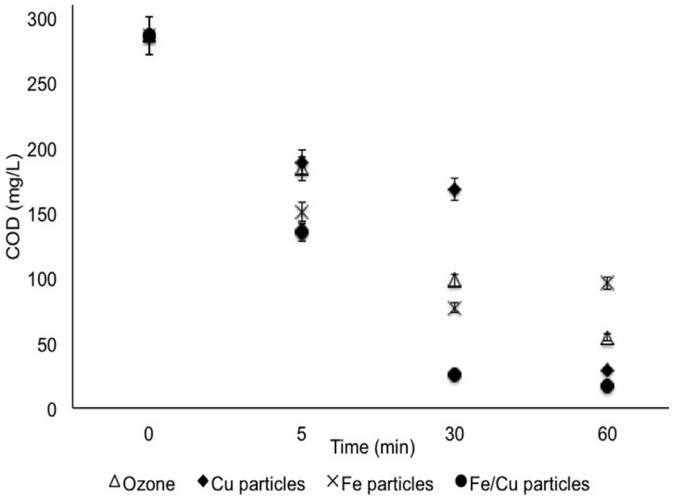

Fig. 6. Effect of time and catalyst type on Chemical Oxygen Demand (COD).

In the above reactions, the kinetic constants as previously reported [33,35–37] were also included. It can be observed that the production of oxidant radicals is about three orders of magnitude higher through Fenton like than through the Fenton process. This can explain the differences observed in the concentration profiles of both, the IC and the ISA, shown in Fig. 5. From data shown in Fig. 5a, the initial IC reaction rate ($-r_{IC0}$) was obtained and the results are presented in Table 1. It is confirmed that the fastest IC oxidation process is when the bimetallic system is added. However, it can also be concluded that the oxidation rate with Cu is about twice faster than when adding Fe particles and this can be ascribed to the kinetics of reactions 18–23. Moreover, the relatively low concentration of ISA observed in Fig. 5b when ozonation is catalyzed with Cu, confirms that hydroxyl radicals are faster produced and therefore consumed in the further oxidation of ISA with Cu than with Fe particles. This is in concordance with the measurements of Chemical Oxygen.

Demand (Fig. 6) and Total Organic Carbon after 60 min of reaction (Table 2). The observed improvement when adding bimetallic particles may be explained by acknowledging reactions 2–26, *i.e.* •OH radicals are simultaneously produced by ozonation, peroxonation, Fenton and Fenton-like reactions. Furthermore, by contrasting the concentration profiles shown in Fig. 5, it can be concluded that the use of the bimetallic system not only enhances the degradation of the IC molecule but also positively affects the degradation of ISA. Nevertheless, the ISA is not fully oxidized by any of the studied systems at the essayed reaction time. As expected from these results, the Chemical Oxygen Demand (COD) (Fig. 6) nor the TOC values (Table 2) are zero for any of the studied treatments. However, through an insightful analysis of Figs. 5 and 6, it can be inferred that at lower ISA concentrations, ozone and cupper rather promote the oxidation of ISA byproducts than the ISA oxidation. This can be stated since during both processes, ozone alone and $O_3 + Cu$, the reaction rate of ISA between 10 and 60 min is practically zero (Fig. 5) while the COD diminishing rate is evident (Fig. 6) during the same period of time. Hence, since no change in ISA concentration is evident during this time, the change of COD can be ascribed to both, the reduction of IC concentration and to the further oxidation of the produced carboxylic acids, *i.e.* oxalic and oxamic acid. The presence of these compounds as ISA oxidation products has been previously reported [11]. Samples TOC values after 60 min of reaction for each treatment where established and are presented in Table 2. It can be concluded that after 60 min of reaction, full mineralization (reaction 26) is not achieved with none of the studied systems as already suggested by the shown results in Figs. 5 and 6. The use of the bimetallic system Fe/Cu, however, leads to the maximum mineralization degree of the treated solution (a final value of 13 mg/l was achieved). It is worth pointing out that according to NOM-014-CONAGUA-2003, a maximum of 16 mg/l of TOC is required for artificial recharge with treated waste water. It is also worth noticing that Fe is the less effective metallic system to oxidize ISA and hence to remove organic carbon. This may be due to the easiness of Fe to be oxidized by reactions 14, 18 and 20. In addition, reactions 18 and 20 may occur more rapidly than reaction 20 by which the active specie Fe^{2+} is regenerated.

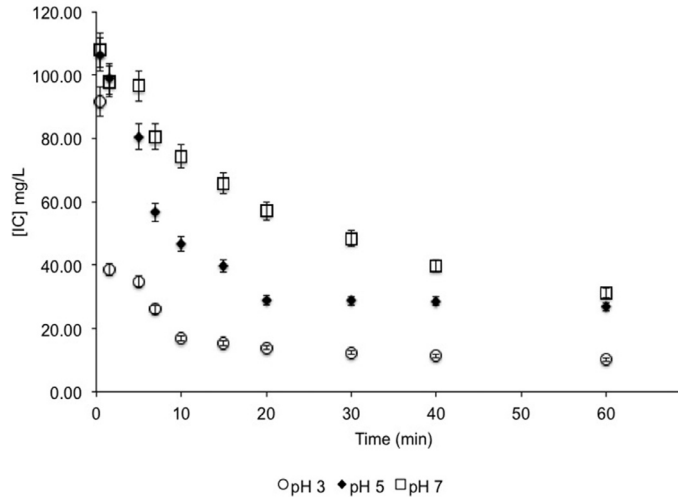

Fig. 7. Effect of pH on IC degradation reaction.

3.4. Effect of pH on the degradation of IC

Because of effectiveness reasons, the effect of pH was only evaluated when Fe/Cu particles were added to the ozonation treatment. The effect of this variable was evaluated at pH values of 3, 5 and 7. Alkaline pH values were avoided in order to reduce the formation of hydroxides and oxides. Fig. 7 shows that the degradation efficiency increased when decreasing pH, and a maximum efficiency (97%) was observed at pH 3 after only 10 min of treatment. This behavior can be related to the highest generation rate of the main oxidant •OH via Fenton (reactions 18–21) and Fenton like reactions (reactions 22 and 23), since its optimum pH is 2.8 [37], very close to pH 3.0 where indigo carmine and its products are more rapidly destroyed.

4. Conclusions

By a chemical reduction method, the synthesis of Fe^{2+}, Cu^{2+} and Fe^{2+}/Cu^{2+} particles were possible. The effect of these materials on the IC degradation by ozonation was established. The bimetallic system Fe/Cu was the most efficient in terms not only of IC removal but also regarding by-products oxidation. In the same sense, it can be stated that Fe is the less effective material. At all cases, a catalytic effect cannot be neglected through Fenton and Fenton-like reactions. pH is a variable of paramount importance in the ozonation process. The highest mineralization degree (94%) and COD reduction (95%) of the IC solution was achieved after 10 min of ozonation under pH 3, ozone dose of 0.005 g/l, 1000 mg/l of Fe/Cu.

Acknowledgments

The authors wish to acknowledge the financial support of PRODEP through project (103.5/13/5257). Teresa Torres Blancas acknowledges the scholarship from CONACyT to pursue her postgraduate degree. We thank M.Sc. Virginia Gómez Vidales for technical assistance.

Supplementary materials

Supplementary material associated with this article can be found, in the online version, at doi:10.1016/j.jtice.2017.02.025.

References

[1] Majcen A, Marechal L, Križanec B. Textile Finishing Industry as an Important Source of Organic Pollutants n.d.
[2] Song S, Yao J, He Z, Qiu J, Chen J. Effect of operational parameters on the decolorization of C.I. Reactive Blue 19 in aqueous solution by ozone-enhanced electrocoagulation. J Hazard Mater 2008;152:204–10.
[3] Cañizares P, Martínez F, Jiménez C, Lobato J, Rodrigo MA. Coagulation and electrocoagulation of wastes polluted with dyes. Environ Sci Technol 2006;40:6418–24.
[4] Vandevivere PC, Bianchi R, Verstraete W. Treatment and reuse of wastewater from the textile wet-processing industry: review of emerging technologies. J Chem Technol Biotechnol 1998;72:289–302.
[5] Verma AK, Dash RR, Bhunia P. A review on chemical coagulation/flocculation technologies for removal of colour from textile wastewaters. J Environ Manag 2012;93:154–68.
[6] Bes-Piá A, Mendoza-Roca JA, Alcaina-Miranda MI, Iborra-Clar A, Iborra-Clar MI. Reuse of wastewater of the textile industry after its treatment with a combination of physico-chemical treatment and membrane technologies. Desalination 2002;149:169–74.
[7] Wade Miller G. Integrated concepts in water reuse: managing global water needs. Desalination 2006;187:65–75.
[8] Gandra N, Frank AT, Le Gendre O, Sawwan N, Aebisher D, Liebman JF, et al. Possible singlet oxygen generation from the photolysis of indigo dyes in methanol, DMSO, water, and ionic liquid, 1-butyl-3-methylimidazolium tetrafluoroborate. Tetrahedron 2006;62:10771–6.
[9] Kim TH, Lee Y, Yang J, Lee B, Park C, Kim S. Decolorization of dye solutions by a membrane bioreactor (MBR) using white-rot fungi. Desalination 2004;168:287–93.
[10] Tantak NP, Chaudhari S. Degradation of azo dyes by sequential Fenton's oxidation and aerobic biological treatment. J Hazard Mater 2006;136:698–705.
[11] Flox C, Ammar S, Arias C, Brillas E, Viridiana, A, Vargas-Zavala RA. Electro-Fenton and photoelectro-Fenton degradation of indigo carmine in acidic aqueous medium. Appl Catal B Environ 2006;67:93–104.
[12] Bernal M, Romero R, Roa G, Barrera-Díaz C. Teresa Torres-Blancas and RN. Ozonation of indigo carmine catalyzed with Fe-pillared clay. Int J Photoenergy 2013:7.
[13] Song S, He Z, Qiu J, Xu L, Chen J. Ozone assisted electrocoagulation for decolorization of C.I. Reactive Black 5 in aqueous solution: An investigation of the effect of operational parameters. Sep Purif Technol 2007;55:238–245.
[14] Kwan WP, Voelker BM. Influence of electrostatics on the oxidation rates of organic compounds in heterogeneous Fenton systems. Environ Sci Technol 2004;38:3425–31.
[15] Kwan WP, Voelker BM. Rates of hydroxyl radical generation and organic compound oxidation in mineral-catalyzed Fenton-like systems. Environ Sci Technol 2003;37:1150–8.
[16] Xia M, Long M, Yang Y, Chen C, Cai W, Zhou B. A highly active bimetallic oxides catalyst supported on Al-containing MCM-41 for Fenton oxidation of phenol solution. Appl Catal B Environ 2011;110:118–25.
[17] Al-shamsi MA, Thomson NR, Forsey SP. Iron based bimetallic nanoparticles to activate peroxygens. Chem Eng J 2013;232:555–63.
[18] Bokare AD, Chikate RC, Rode CV, Paknikar KM. Iron-nickel bimetallic nanoparticles for reductive degradation of azo dye Orange G in aqueous solution. Appl Catal B Environ 2008;79:270–8.
[19] O'Carroll D, Sleep B, Krol M, Boparai H, Kocur C. Nanoscale zero valent iron and bimetallic particles for contaminated site remediation. Adv Water Resour 2013;51:104–22.
[20] Liu W-J, Qian T-T, Jiang H. Bimetallic Fe nanoparticles: recent advances in synthesis and application in catalytic elimination of environmental pollutants. Chem Eng J 2014;236:448–63.
[21] Dong Y, Han Z, Dong S, Wu J, Ding Z. Enhanced catalytic activity of Fe bimetallic modified PAN fiber complexes prepared with different assisted metal ions for degradation of organic dye. Catal Today 2011;175:299–309.
[22] Sridharan K, Endo T, Cho S, Kim J, Joo T, Philip R. Single step synthesis and optical limiting properties of Ni–Ag and Fe–Ag bimetallic nanoparticles. Opt Mater 2013;35:860–7.
[23] Flox C, Ammar S, Arias C, Brillas E, Viridiana A, Vargas-Zavala RA, et al. Electro-Fenton and photoelectro-Fenton degradation of indigo carmine in acidic aqueous medium. Appl Catal B Environ 2006;67:93–104.
[24] Ammar S, Abdelhedi R, Flox C, Arias C, Brillas E. Electrochemical degradation of the dye indigo carmine at boron-doped diamond anode for wastewaters remediation. Environ Chem Lett 2006;4:229–33.
[25] Torres-Blancas T, Roa-Morales G, Barrera-Díaz C, Ureña-Núñez F, Cruz-Olivares J, Balderas-Hernandez P, et al. Ozonation of indigo carmine enhanced by Fe/Pimenta dioica L. Merrill particles. Int J Photoenergy 2015;2015:9 Article ID 608412.
[26] Liu X, Chen Z, Chen Z, Megharaj M, Naidu R. Remediation of Direct Black G in wastewater using kaolin-supported bimetallic Fe/Ni nanoparticles. Chem Eng J 2013;223:764–71.
[27] J.E. Wertz, J.R. Bolton. Electron spin resonance: elementary theory and practical applications. John Wiley & Sons, Inc.
[28] APHA, AWWA and WEF. Standard Methods for the Examination of Water and Wastewater, American Public Health Association (APHA), American Water Works Association (AWWA) & Water Environment Federation (WEF). 21st Edition, NY, USA; 2005.
[29] Shu HY, Chang MC, Yu HH, Chen WH. Reduction of an azo dye Acid Black 24 solution using synthesized nanoscale zerovalent iron particles. J Colloid Interface Sci 2007;314:89–97.

[30] Garribba E, Micera G. The determination of the geometry of Cu(II) complexes: an EPR spectroscopy experiment. J Chem Educ 2006;83:1229.
[31] Quiroz AC, Barrera-díaz C, Roa-morales G, Hern PB, Romero R, Natividad R. Wastewater ozonation catalyzed by iron. Ind Eng Chem Res 2011:2488–94.
[32] Sirés I, Garrido JA, Rodríguez RM, Cabot PL, Centellas F, Arias C, et al. Electrochemical degradation of paracetamol from water by catalytic action of Fe2+, Cu2+, and UVA light on electrogenerated hydrogen peroxide. J Electrochem Soc 2006;153.
[33] Chandrasekara Pillai K, Kwon TO, Moon IS. Degradation of wastewater from terephthalic acid manufacturing process by ozonation catalyzed with F^{e2+}, H_2O_2 and UV light: direct versus indirect ozonation reactions. Appl Catal B Environ 2009;91:319–28.
[34] Sutton HC. Formate oxidation induced by a copper peroxo complex produced in Fenton-like reactions. J Chem Soc Faraday Trans 1 Phys Chem Condens Ph. 1989;85:883.
[35] Comninellis C, Chen G. Electrochemistry for the environment. New York Dordrecht Heidelberg London: Springer; 2010.
[36] Bach A, Shemer H, Semiat R. Kinetics of phenol mineralization by Fenton-like oxidation. Desalination 2010;264:188–92.
[37] Bokare AD, Choi W. Review of iron-free Fenton-like systems for activating H_2O_2 in advanced oxidation processes. J Hazard Mater 2014;275:121–35.